Report

Neuron

Netrin1 Produced by Neural Progenitors, Not Floor Plate Cells, Is Required for Axon Guidance in the Spinal Cord

Highlights

- Netrin1 signaling from the VZ, not the FP, guides spinal commissural axons
- Spinal progenitors produce netrin1 and deposit it as a substrate on the pial surface
- The VZ-derived netrin1 substrate promotes ventrally directed axonal growth
- Dcc is required to interpret the axonal response to VZ-derived netrin1

Authors

Supraja G. Varadarajan, Jennifer H. Kong, Keith D. Phan, ..., Artur Kania, Bennett G. Novitch, Samantha J. Butler

Correspondence

butlersj@ucla.edu

In Brief

Varadarajan et al. show that netrin1 supplied by neural progenitors, not floor plate (FP) cells, guides commissural axons in the developing spinal cord. These findings contrast with the long-held model that the FP supplies a long-range axonal chemoattractant. Rather, netrin1 is produced by neural progenitors and deposited on the pial surface, providing a growth substrate that directs ventrally directed axonal growth.

Varadarajan et al., 2017, Neuron *94*, 790–799
May 17, 2017
http://dx.doi.org/10.1016/j.neuron.2017.03.007

CellPress

CellPress

Neuron
Report

Netrin1 Produced by Neural Progenitors, Not Floor Plate Cells, Is Required for Axon Guidance in the Spinal Cord

Supraja G. Varadarajan,[1,2,3] Jennifer H. Kong,[1,2,3] Keith D. Phan,[1,2] Tzu-Jen Kao,[4,5] S. Carmen Panaitof,[6] Julie Cardin,[5] Holger Eltzschig,[7] Artur Kania,[4,8,9] Bennett G. Novitch,[1,2,3] and Samantha J. Butler[1,2,3,10,*]

[1]Department of Neurobiology
[2]Eli and Edythe Broad Center of Regenerative Medicine and Stem Cell Research
[3]Neuroscience Interdisciplinary Graduate Program
University of California, Los Angeles, Los Angeles, CA 90095, USA
[4]Institut de Recherches Cliniques de Montréal, 110 Avenue des Pins Ouest, Montréal, QC H2W 1R7, Canada
[5]Graduate Institute of Neural Regenerative Medicine, College of Medical Science and Technology and Center for Neurotrauma and Neuroregeneration, Taipei Medical University, Taipei, Taiwan
[6]Department of Biology, University of Nebraska, Kearney, Kearney, NE 68849, USA
[7]Department of Anesthesiology, The University of Texas Health Science Center at Houston, McGovern Medical School, Houston, TX 77030, USA
[8]Faculté de Médecine, Université de Montréal, Montréal, QC H3C 3J7, Canada
[9]Departments of Anatomy and Cell Biology and Biology, Division of Experimental Medicine, McGill University, Montréal, QC H3A 3R1, Canada
[10]Lead Contact
*Correspondence: butlersj@ucla.edu
http://dx.doi.org/10.1016/j.neuron.2017.03.007

SUMMARY

Netrin1 has been proposed to act from the floor plate (FP) as a long-range diffusible chemoattractant for commissural axons in the embryonic spinal cord. However, netrin1 mRNA and protein are also present in neural progenitors within the ventricular zone (VZ), raising the question of which source of netrin1 promotes ventrally directed axon growth. Here, we use genetic approaches in mice to selectively remove netrin from different regions of the spinal cord. Our analyses show that the FP is not the source of netrin1 directing axons to the ventral midline, while local VZ-supplied netrin1 is required for this step. Furthermore, rather than being present in a gradient, netrin1 protein accumulates on the pial surface adjacent to the path of commissural axon extension. Thus, netrin1 does not act as a long-range secreted chemoattractant for commissural spinal axons but instead promotes ventrally directed axon outgrowth by haptotaxis, i.e., directed growth along an adhesive surface.

INTRODUCTION

The establishment of neural circuits during development requires neurons to extend axons along precise pathways toward their synaptic targets. Axons can navigate over considerable distances, using molecular cues in the embryonic environment to both spatially and temporally orient their growth cones (Butler and Tear, 2007; Phan et al., 2010). These guidance cues have been proposed to fall into four major categories: attractive or repulsive signals that act as either long-range diffusible molecules or short-range contact-dependent signals, i.e., tethered to a cellular membrane or the extracellular matrix (ECM) (Tessier-Lavigne and Goodman, 1996). Particular attention has been placed on identifying diffusible cues from "guidepost" source cells, which could direct axonal growth cones over long distances.

The textbook example of a chemotropic guidance factor is netrin1, a member of the laminin superfamily first characterized in the vertebrate spinal cord (Kennedy et al., 1994; Serafini et al., 1994). Studies in chicken and mouse led to the proposal that netrin1 emanates from the floor plate (FP) and acts as a diffusible chemoattractant to direct the ventral growth of spinal commissural axons (Kennedy et al., 1994). Considerable work using soluble netrin1 in in vitro assays supported the hypothesis that it can act at a distance to orient axon growth (de la Torre et al., 1997; Ming et al., 1997; Sloan et al., 2015). However, subsequent investigation in other systems, including angiogenesis and retinal, pancreatic, and mammary gland development, have indicated that netrin1 acts between cells and the ECM, to regulate cell adhesion and tissue morphogenesis (Lai Wing Sun et al., 2011). Notably, studies in the *Drosophila* nerve cord and visual system have shown that membrane-tethered netrin was sufficient to rescue axon guidance defects in *netrinA/B* mutants (Brankatschk and Dickson, 2006; Timofeev et al., 2012). Recently, studies using live imaging in the visual system have demonstrated that target-derived netrin1 is required to attach growth cones to source cells (Akin and Zipursky, 2016). However, despite significant progress understanding netrin-mediated axon guidance, it has not been resolved whether netrin1 acts from the FP as a diffusible chemoattractant in vivo.

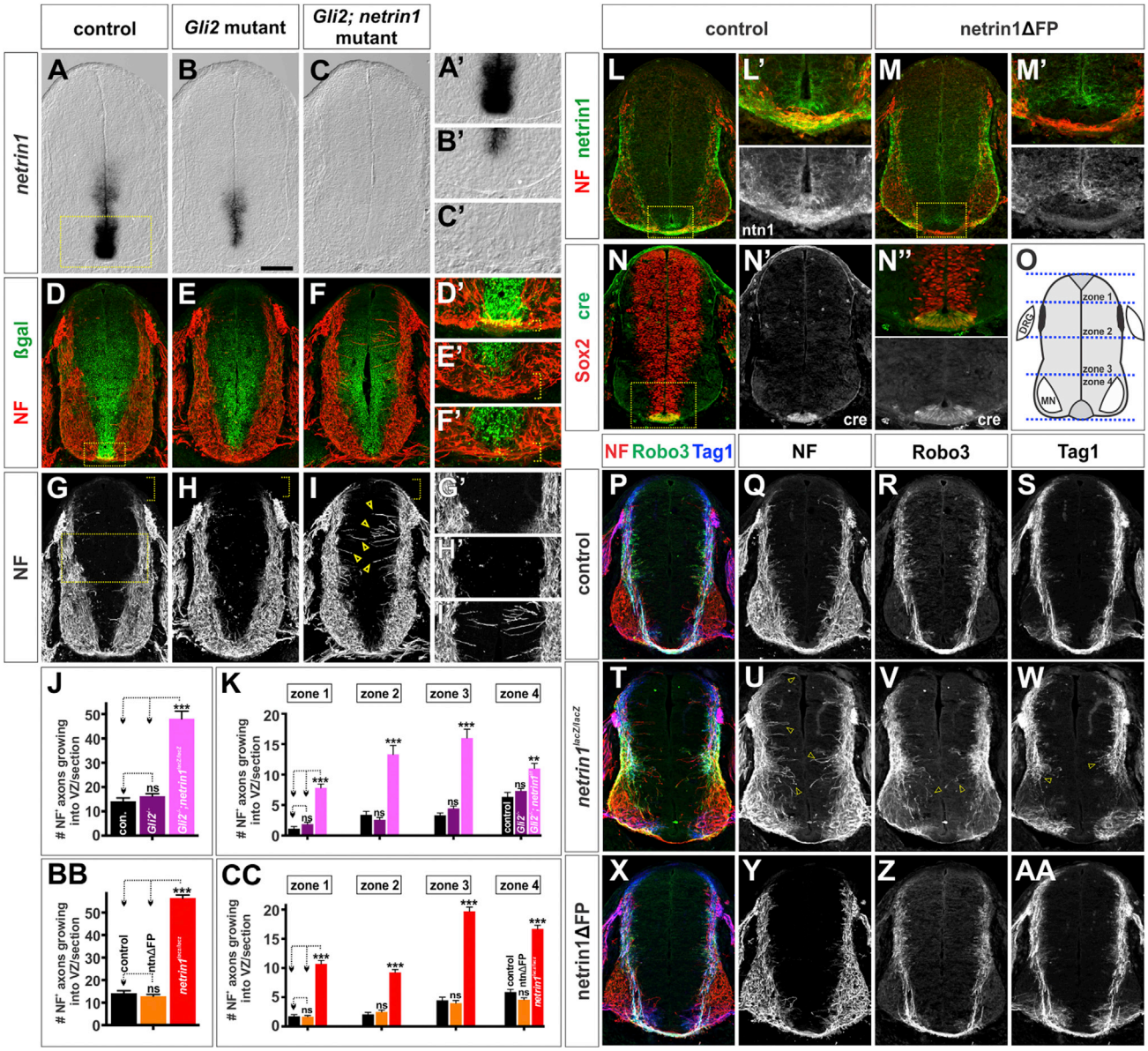

Figure 1. FP-Derived Netrin1 Is Not Required to Direct the Circumferential Trajectory of Spinal Axons

(A–I and L–AA) Thoracic level transverse sections from E11.5 *netrin1*$^{lacZ/+}$; *Gli2*$^{+/-}$ (control, A, D, and G), *netrin1*$^{lacZ/+}$; *Gli2*$^{-/-}$ (*Gli2* mutant, B, E, and H), *netrin1*$^{lacZ/lacZ}$; *Gli2*$^{-/-}$ (*netrin1*; *Gli2* mutant, C, F, and I), Shh::*cre*; *netrin1*$^{flox/+}$ (control, L, N, and P–S), Shh::*cre*; *netrin1*$^{flox/flox}$ (netrin1ΔFP M, X–AA), and *netrin1*$^{lacZ/lacZ}$ (T–W) mouse spinal cords.

(A–C′) *Netrin1* expression is specifically lost from the FP in *Gli2* mutants (B, FP region is shown magnified in A′–C′) and is completely absent from *Gli2; netrin1* mutants.

(D–I′) NF$^+$ axons grow circumferentially in control and *Gli2* mutants avoiding the netrin1::β-gal$^+$ VZ (G′ and H′). In contrast, NF$^+$ axons extend robustly into the VZ in the *Gli2; netrin1* mutants (arrows, I′).

(J, K, and O) Quantification showed that there are 2- to 3-fold more NF$^+$ axons extending toward the VZ in the *Gli2; netrin1* mutants (48.1 ± 3.1 NF$^+$ axons/section; n = 26 sections from 2 embryos) compared to either control (14.2 ± 1.4 NF$^+$ axons/section; n = 26 sections from 2 embryos) or *Gli2* mutants (16.2 ± 1.0 NF$^+$ axons/section; n = 50 sections from 4 embryos). *Gli2; netrin1* mutant axons extend aberrantly into the VZ in all zones of the spinal cord (O).

(L–M′) Netrin1 is specifically lost from the FP in the netrin1ΔFP mice compared to control (FP region magnified in L′ and M′).

(N–N′′) Cre is only present in FP cells in both control and netrin1ΔFP embryos (FP region magnified in N′′).

(O) Quantification schematic of four zones along the dorsal-ventral axis of the spinal cord.

(P–AA) The NF$^+$, Tag1$^+$ and Robo3$^+$ populations of axons project apparently normally around the VZ in netrin1ΔFP spinal cords (X–AA), very similar to littermate controls (P–S) and distinct from the multiple phenotypes observed in *netrin1*$^{lacZ/lacZ}$ mutants (T–W) (Laumonnerie et al., 2015; Serafini et al., 1996).

(BB and CC) Quantification demonstrated that there is no significant difference ($p > 0.31$) between the number of NF$^+$ axons extending toward the VZ in control (14.2 ± 1.1 NF$^+$ axons/section; n = 53 sections from 3 embryos) and netrin1ΔFP (12.8 ± 0.8 NF$^+$ axons/section; n = 67 sections from 4 embryos) mice. In contrast,

(legend continued on next page)

In the mouse spinal cord, *netrin1* is expressed by neural progenitors in ventricular zone (VZ), in addition to the FP (Serafini et al., 1996). Moreover, netrin1 protein has a complex distribution that does not fit the model of a simple continuous gradient emanating from the FP (Kennedy et al., 2006). In this study, we set out to determine which source of netrin1 in the spinal cord directs axonal growth to the FP. To resolve this question, we used conditional genetic approaches in mouse to remove netrin1 expression from either the VZ or the FP. In the absence of either netrin1 or Dcc, spinal axons aberrantly innervate the VZ and commissural axons either stall or are dramatically defasciculated. However, these phenotypes are only observed when netrin1 is ablated from the VZ, but not the FP. We thus demonstrate that the key source of netrin1 supplying guidance activities comes from neural progenitors in the VZ, rather than the FP as previously suggested. Our studies further demonstrate that the cellular geometry of spinal neural progenitors permits the establishment of a netrin1^{+} growth substrate along the pial surface of the spinal cord, which acts to position and promote fasciculated spinal axon outgrowth, in a Dcc-dependent manner. Thus, rather than acting as a soluble diffusible molecule produced by the FP, we propose that netrin1 promotes ventrally directed axon outgrowth in the spinal cord by haptotaxis, the directed growth of cells along an adhesive surface (Carter, 1965).

RESULTS

FP-Derived Netrin1 Is Not Required for Commissural Axon Guidance to the FP

The canonical model for netrin1 function in the spinal cord suggests that netrin1 acts as a diffusible chemoattractant emanating from the FP (Serafini et al., 1996). However, *netrin1* transcript is also expressed by many progenitors in the VZ in the mouse spinal cord (Serafini et al., 1996), a region ubiquitously avoided by spinal axons (Figures S1A–S1D) (Butler and Bronner, 2015). To resolve the role of FP- versus VZ-derived netrin1, we have used multiple genetic approaches to determine the spatial requirement for netrin1 in the developing spinal cord.

First, we assessed the consequence of anatomically deleting the FP on the trajectory of neurofilament (NF)$^{+}$ spinal axons in embryonic day 11.5 (E11.5) mouse embryos. Gli2 is a key transcriptional regulator that transduces sonic hedgehog (Shh) signaling (Matise et al., 1998). The FP and V3 interneurons are ablated in *Gli2*$^{-/-}$ mutants, resulting in the loss of FP-derived netrin1 (Figures 1A′, 1B′, 1D′, and 1E′) (Matise et al., 1998). Critically for our studies, the VZ expression of *netrin1* is largely unaffected in *Gli2*$^{-/-}$ mutants (Figure 1B). In contrast, *netrin1* expression is lost from the VZ in *Gli2; netrin1* double mutants (Figure 1C). Strikingly, the absence of the FP has no significant effect on the trajectory of NF^{+} axons, they continue to ubiquitously avoid the VZ in similar numbers to control littermates ($p > 0.22$, Figures 1D, 1E, 1G′, 1H′, 1J, and 1K) (Kadison et al., 2006; Matise et al., 1999). In contrast, NF^{+} axons robustly extend into the VZ in *Gli2*$^{-/-}$*; netrin1*$^{lacZ/lacZ}$ spinal cords (Figures 1F, 1I′–1K), in comparable numbers to those observed in *netrin1*$^{lacZ/lacZ}$ single mutants (Figures 1BB and 1T). Thus, NF^{+} axon guidance defects are only observed in the absence of VZ-derived netrin1.

Second, we conditionally ablated netrin1 from the FP (netrin1ΔFP) using the Shh::*cre* driver line (Harfe et al., 2004) in combination with a *netrin1*$^{flox/flox}$ allele (Brunet et al., 2014). In these mice, the presence of cre in the FP (Figures 1N–1N″) results in the specific loss of netrin1 protein from the FP (Figures 1L–1M′). Remarkably, this manipulation resulted in no significant disruption in axonal growth (Figures 1X–1AA). In particular, both Tag1^{+} and Robo3^{+} commissural spinal axons project normally around the VZ and across the FP, in tightly fasciculated bundles, in a manner similar to control littermates (Figures 1P–1S, 1BB, and 1CC; $p > 0.31$). This result is in contrast to the previously characterized loss-of-function allele of netrin1 (*netrin1*$^{lacZ/lacZ}$), which shows multiple perturbations in axon growth: first, many NF^{+} axons grow medially into the VZ (arrows, Figures 1U, 1BB–1CC, S1E and S1G), second, Robo3^{+} commissural axons are profoundly defasciculated (Figures 1V, S1F and S1H) (Laumonnerie et al., 2015), and third, Tag1^{+} commissural axons stall above the developing motor column (Serafini et al., 1996) (arrows, Figure 1W). Taken together, these findings indicate that the commissural axon defects previously observed in *netrin1* mutants do not arise from the loss of netrin1 from the FP.

VZ-Derived Netrin1 Is Necessary for Axon Guidance to the FP

We next sought to examine whether the selective loss of netrin1 from the VZ could recapitulate the axon guidance defects seen in *netrin*$^{lacZ/lacZ}$ mutants. Toward this goal, we removed netrin1 from all dorsal spinal progenitors (netrin1ΔdVZ) by recombining the *netrin1*$^{flox/flox}$ allele with a Pax3::*cre* driver line (Lang et al., 2005) (Figure 2C). Netrin1 protein decorates both the pial surface of the spinal cord, as well as commissural axons (Kennedy et al., 2006; MacLennan et al., 1997). Following cre recombination, netrin1 is specifically ablated from the dorsal pial surface and axons extending within the dorsal spinal cord (Figures 2A and 2D), repositioning these axons laterally such that they contact the laminin^{+} basement membrane (Figures 2B and 2E). Netrin1 levels in the netrin1ΔdVZ FP are comparable to those seen in control littermates (Figures 2F and 2G).

The netrin1ΔdVZ manipulation resulted in many guidance phenotypes similar to those observed in *netrin1*$^{lacZ/lacZ}$ embryos. NF^{+} axons aberrantly grow both dorsally toward the RP and medially into the dorsal VZ (Figures 2H, 2L, and 2P–2S). Robo3^{+} commissural axons are also significantly defasciculated compared to control littermates (Figures 2J, 2N, 2T, and 2U). Interestingly, the extent of defasciculation is not as profound as is observed for *netrin1*$^{lacZ/lacZ}$ embryos (Figures S1F and S1H), perhaps because netrin1 belatedly accumulates on axons as they grow into the ventral netrin1^{+} region (arrows, Figure 2D). Nonetheless,

NF^{+} axons profusely project into the VZ in *netrin1*$^{lacZ/lacZ}$ mutant embryos (56.4 ± 1.4 NF^{+} axons/section; n = 68 sections from 6 embryos) at all zones of the spinal cord (O).

Data are represented as mean ± SEM. Probability of similarity $^{**}p < 0.005$, $^{***}p < 0.0005$, Student's t test. Scale bar is represented as 140 μm in (A)–(C) and as 105 μm in (D)–(I) and (L)–(AA).

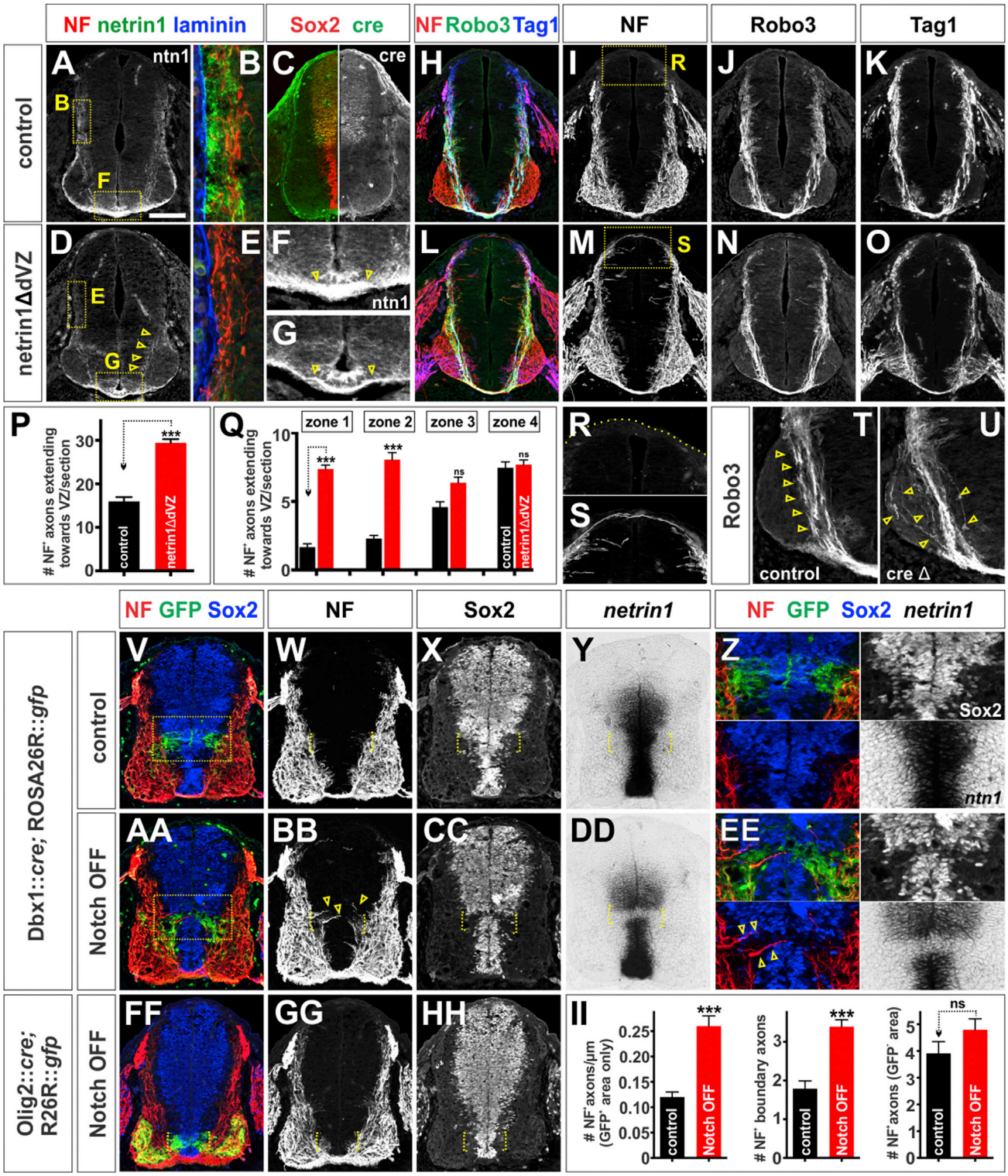

Figure 2. Selective Depletion of Netrin1 from the VZ Results in Axon Guidance Defects

(A–U and V–HH) Thoracic level transverse sections of E11.5 Pax3::*cre*; *netrin1*$^{flox/+}$ (control, A–C, F, H–K, R, and T), Pax3::*cre*; *netrin1*$^{flox/flox}$ (netrin1ΔdVZ, D and E, G, L–O, S, and U), Dbx1::*cre*; ROSA26R::*gfp* (control, V–Z), Dbx1::*cre*; *Rbpj*$^{flox/flox}$; ROSA26R::*gfp* (Notch OFF, AA–EE), and Olig2::*cre*; *Rbpj*$^{flox/flox}$; ROSA26R::*gfp* (Notch OFF, FF–II) mouse spinal cords.

(legend continued on next page)

fewer netrin1$^+$ axons appear to cross the FP (arrows, Figures 2F and 2G). Tag1$^+$ axon growth is also diminished, such that fewer Tag1$^+$ fascicles extend to the FP in the netrin1ΔdVZ mutants compared to littermate controls (Figures 2K and 2O).

We also examined the consequence of a smaller deletion in *netrin1* expression by focally disrupting neural progenitor maintenance. We used a Dbx1::*cre* driver line to functionally inactivate Rbpj, the key transcriptional effector of the Notch signaling pathway, specifically in the p0 progenitor domain (Notch OFF; Kong et al., 2015). We used a ROSA26R::*gfp* reporter line to simultaneously lineage trace Dbx1$^+$ cells (Figures 2V and 2AA). As previously reported (Kong et al., 2015), silencing Notch signaling in p0 progenitors results in the loss of Sox2 and other neural progenitor characteristics including *netrin1* expression (brackets, Figures 2X–2Z and 2CC–2EE). This manipulation creates two ectopic boundaries of *netrin1* expression not seen in controls (brackets, Figures 2Y and 2DD). The distribution of pial-associated netrin1 is not significantly affected by this manipulation (data not shown). Nevertheless, >2-fold more NF$^+$ axons grow into the Notch OFF GFP$^+$ region (arrows, Figure 2EE), with many axons precisely following along the edge of the ectopic *netrin1* boundaries (brackets, Figures 2W, 2BB, 2EE, and 2II).

This axon growth phenotype does not result as a secondary consequence of inactivating Notch: conditionally ablating Rbpj from the pMN alters progenitor patterning (Kong et al., 2015) but does not disrupt the expression of Sox2 (Figures 2FF and 2HH) or *netrin1* expression (data not shown). Consistent with these findings, NF$^+$ axon trajectories were not affected by this manipulation (brackets, Figures 2GG and 2HH). Collectively, these experiments demonstrate that the axonal growth defects observed in *netrin1* mutants are due to the loss of netrin1 derived from the VZ, not the FP.

Neural Progenitors Establish a Netrin1$^+$ Growth Substrate on the Pial Surface of the Spinal Cord

We next explored the role that VZ-derived netrin1 plays guiding spinal axons. Previous studies have suggested that there is a key difference between the distribution of *netrin1* transcript, which can be detected by in situ hybridization or genetically encoded β-galactosidase (β-gal) from the *netrin1^{lacZ}* reporter line (Serafini et al., 1996), and netrin1 protein (Kennedy et al., 2006). While *netrin1* transcript is made by neural progenitors in the VZ (Figures 3A and 3B), netrin1 protein decorates the laminin$^+$ pial surface (Figure 3C) and commissural axons (chevrons, Figure 3C′). We observed a striking coincidence between the presence of netrin1 at the pial surface and the dorsal boundary of *netrin1* expression in the VZ (dotted lines, Figures 3A–3C). This alignment suggests that netrin1 is produced by bipolar neural progenitors and then transported via their nestin$^+$ radial processes to the basement membrane where their endfeet contact the laminin$^+$ pial surface (Hockfield and McKay, 1985). Supporting this hypothesis, we are unable to detect netrin1 protein in the dorsal-most spinal cord (Figures 3D–3F), further suggesting that there is limited or no diffusion of netrin1. In the intermediate spinal cord, netrin1 protein can be readily detected in nestin$^+$ fibers (Movie S1) and endfeet as they contact the basal pial surface (arrows, Figure 3H). Netrin1 is also co-localized with laminin on the pial surface (Figures 3G and 3I).

There is also a striking correlation between the pattern of spinal axon extension and the domains of *netrin1* transcript and netrin1 protein. From early stages of axiogenesis, NF$^+$ axons appear to preferentially extend immediately adjacent to the netrin1$^+$ pial substrate (Figures 3K and 3K′) and do not innervate the VZ (Figures 3J and 3J′). By E11.5, all axons grow alongside the laminin$^+$ netrin1$^+$ pial substrate in the dorsal-intermediate spinal cord (Figures 3M and 3M′). Tag1$^+$ and Robo3$^+$ axons also project in a fasciculated manner precisely around the netrin1::β-gal$^+$ VZ (Figures 3L and 3M) and then beneath the netrin1::β-gal$^+$ cells in the FP (dotted lines, Figure 3L′). Together with our genetic studies, these data support the model that commissural axon extension is shaped by the polarized deposition of netrin1 at the pial surface.

As commissural axons grow alongside the netrin1$^+$ substrate, they accumulate netrin1 protein (chevrons, Figures 3C′ and 4B). This distribution is not an artifact of our detection methods: netrin1 is completely absent from both the pial surface and axons in *netrin1$^{lacZ/lacZ}$* mutants (Figures 4D–4F). The remaining

(A–G) The Pax3::*cre* line drives expression of cre specifically in the dorsal spinal progenitors (C), resulting in the loss of netrin1 from the dorsal spinal cord of netrin1ΔdVZ embryos (D and E) and not in control littermates (A and B). The NF$^+$ axons move laterally in the netrin1ΔdVZ mice to be immediately adjacent to the laminin$^+$ pial surface (B and E).

(H–K, R, and T) In control littermates, NF$^+$ axons generally avoid the VZ (I) and dorsal-most spinal cord (R), while Robo3$^+$ (J) and Tag1$^+$ (K) commissural axons project in a tightly fasciculated bundle around the VZ and toward the FP (arrows, T).

(L–O) In contrast, there are many axon guidance defects in the netrin1ΔdVZ embryos. NF$^+$ axons extend into the dorsal VZ, with some axons reaching the roof plate (magnified panel in S). Robo3$^+$ axons are defasciculated as they extend ventrally (N, arrows, U), and the number of Tag1$^+$ axons reaching the FP appears to be diminished (O).

(P and Q) Quantification demonstrated that 2-fold more NF$^+$ axons extend toward the VZ in the netrin1ΔdVZ embryos 29.4 ± 0.9 NF$^+$ axons/section; n = 102 sections from 5 embryos) compared to controls (16.0 ± 1.0 NF$^+$ axons/section; n = 64 sections from 3 embryos). These NF$^+$ axons only grew into the VZ in the dorsal zones (i.e., zones 1 and 2), where netrin1 was no longer present, while no significant difference was observed in zones 3 and 4 ($p > 0.11$ and $p > 0.32$, respectively).

(V–Z) The Dbx1::*cre* driver line targets GFP reporter gene expression to the p0 domain (box in V shown magnified in Z).

(AA–EE) The Dbx1::*cre* driver line is used to deplete Notch signaling from p0 domain, the Sox2$^+$ progenitors in this region (brackets, CC) rapidly differentiate into post-mitotic neurons (Kong et al., 2015), which do not express *netrin1* (bracket, DD). NF$^+$ axons now extend around the ectopic netrin1 boundary (arrows, BB).

(FF–HH) Loss of Notch signaling in the Olig2$^+$ pMN domain has no effect on Sox2$^+$ progenitors (bracket, HH) and does not create an ectopic netrin1 boundary or perturb NF$^+$ axon trajectories.

(II) There are >2-fold more NF$^+$ axons/μm entering the VZ in the GFP$^+$ p0 region in the Notch OFF spinal cord compared to controls. Of these, 2-fold more project precisely along the p0 GFP boundary. There was no significant difference ($p > 0.15$) in the number of NF$^+$ axons projecting into the VZ outside the GFP$^+$ p0 region in the Notch OFF and control spinal cords. Control: n = 47 sections from 4 mice; Notch OFF: n = 66 sections from 6 mice.

Data are represented as mean ± SEM. Probability of similarity between control and mutant, ***$p < 0.0005$ Student's t test. Scale bar is represented as 105 μm

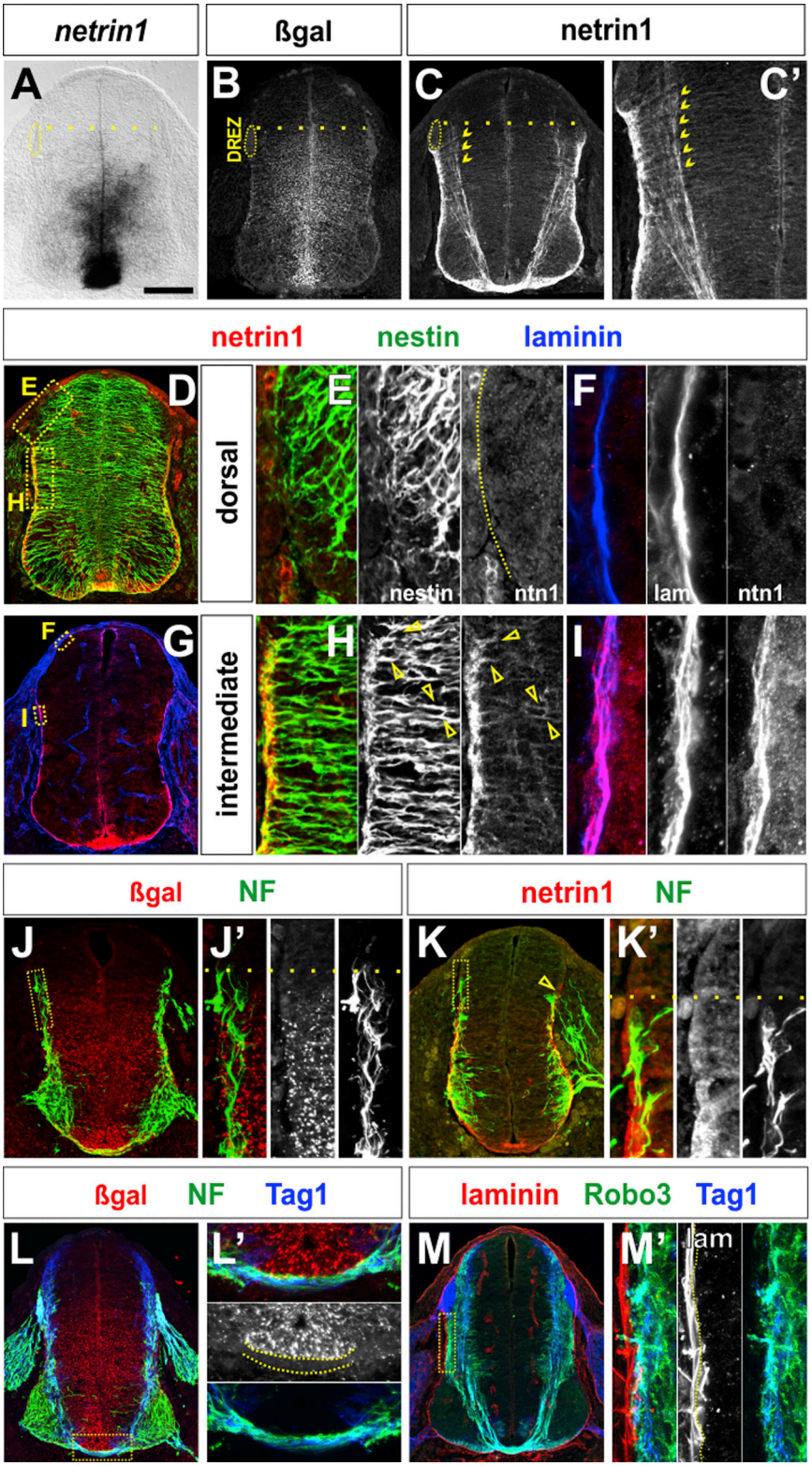

Figure 3. Spinal Progenitors Deposit a Netrin1 Substrate on the Pial Surface

(A–M) E11.5 thoracic (A, B, and L) and lumbar (J) *netrin1*$^{lacZ/+}$ and E10.5 lumbar (K) and E11.5 thoracic (C–G and M) *netrin1*$^{+/+}$ mouse spinal cords. Note that for netrin1 immunohistochemisty, (G) was processed without antigen retrieval.

(A and B) *Netrin1* (A) and netrin1::β-gal (B) are both present in FP cells and neural progenitors in the VZ. The domain of *netrin1* and netrin1::β-gal expression extends from the ventral midline to a dorsal boundary at the same level as the dorsal root entry zone (DREZ, dotted line).

(C and C′) In contrast, high levels of netrin1 protein are observed around the basal pial circumference of the spinal cord starting at the same dorsal boundary observed for *netrin1* expression (dotted line), Netrin1 is also present on commissurally projecting axons (chevrons, C and C′).

(D–I) Netrin1 protein co-localizes with both the nestin^{+} progenitor processes (arrows, H) and the laminin^{+} pial surface (I). Netrin1 is not present at the pial surface in the dorsal-most spinal cord, i.e., above the DREZ, where netrin1::β-gal is not present in the VZ (E and F). See also Movie S1.

(J–K′) NF^{+} axon extension is co-incident with the dorsal border of both netrin1::β-gal expression and netrin1 on the pial surface (dotted line, J′ and K′).

(L and L′) By E11.5, NF^{+} and Tag1^{+} axons project around a continuous border of netrin1::β-gal^{+} cells that spans from the dorsal VZ to the apical FP (dotted lines, L′). Commissural axons are most fasciculated as they project beneath the domain of netrin1::β-gal at the FP (L′).

(L–M′) Axon growth also correlates with distribution of netrin1 protein. NF^{+} axons and Tag1^{+} Robo3^{+} commissural axons extend immediately adjacent to the laminin^{+} netrin1^{+} pial surface in the dorsal spinal cord (M′).

Scale bar is represented as 120 μm.

VZ staining (Figure 4E) stems from the netrin1 antibody recognizing a cytoplasmic truncated netrin1::β-gal fusion product (Poliak et al., 2015; Serafini et al., 1996). Remarkably, we find that the axonal distribution of netrin1 is dependent on Dcc, the receptor thought to mediate chemoattractive responses to netrin1 (Kolodkin and Tessier-Lavigne, 2011). In *Dcc* mutants, netrin1 is present at normal levels on the pial surface, but is greatly reduced in axons (Figures 4G–4I). Together, these results suggest that netrin1 accumulates on commissural axons in a Dcc-dependent manner to promote fasciculated axon growth around the VZ.

Dcc Mediates the Activity of VZ-Derived Netrin1

We further assessed the model that Dcc is required to mediate the activities of pial-associated netrin1 by examining mice mutant for either *Dcc* or members of the *Unc5* family, the receptor complex that mediates the chemorepellent activities of netrin1 (Kolodkin and Tessier-Lavigne, 2011). *Dcc* is

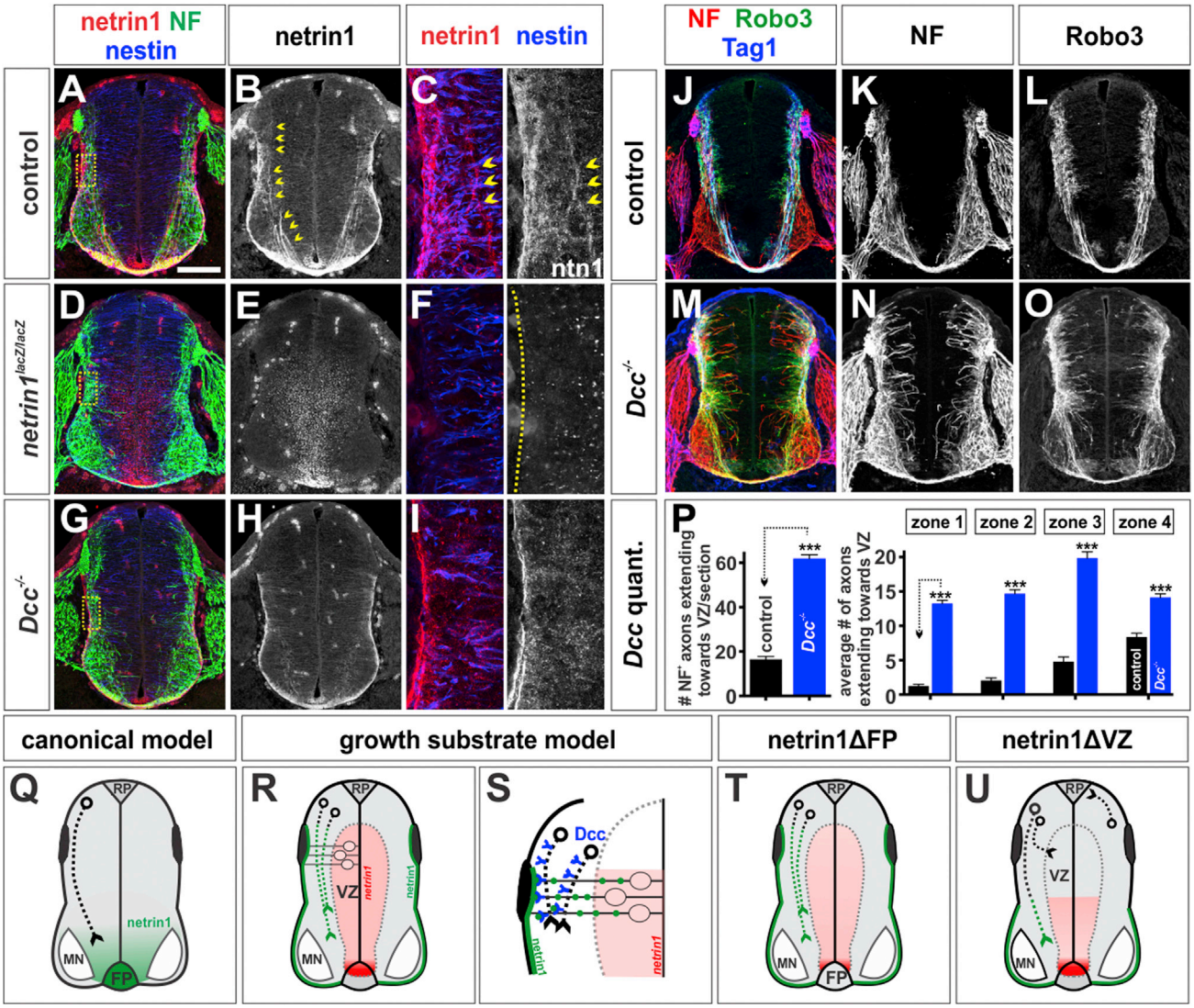

Figure 4. Dcc Mediates the Response to VZ-Derived Netrin1

(A–O) Thoracic level transverse sections of E11.5 *netrin1*$^{+/+}$; *dcc*$^{+/+}$ (control, A–C and J–L) *netrin1*$^{lacZ/lacZ}$ (D–F), and *Dcc*$^{-/-}$ (G–I and M–O) mouse spinal cords.

(A–F) Antigen retrieval (see STAR Methods) boosts the netrin1 signal in axons (chevrons, B and C) and the pial surface (see also Movie S2). This staining is lost in *netrin1*$^{lacZ/lacZ}$ embryos (E and F). As previously described (Poliak et al., 2015), netrin1 antibodies detect the netrin1::β-gal fusion protein in VZ.

(G–I) Netrin1 accumulation in NF^{+} axons is greatly diminished in *Dcc* mutant spinal cords, even though pial-netrin1 remains intact (see also Movie S3).

(J–L) Control NF^{+} (K) and Robo3^{+} (L) axons project precisely around the VZ.

(M–O) In contrast, *Dcc* mutant NF^{+} and Robo3^{+} axons exuberantly project dorsally into the VZ at all levels (N and O). Robo3^{+} axons are also profoundly defasciculated in the motor columns (O).

(P) Quantification of the average number of NF^{+} axons extending into the VZ demonstrates that a comparable number of NF+ axons extend into the VZ in *Dcc* and *netrin1* (Figures 1BB and 1CC) mutant embryos. Control: n = 44 sections, 3 embryos, and *Dcc*$^{-/-}$: n = 105 sections, 6 embryos.

(Q) In the canonical model, netrin1 functions as a long-range chemoattractant secreted by cells in the FP.

(R and S) In the growth substrate model, netrin1 produced by neural progenitors is transported to the pial surface in their radial processes to form a growth substrate (green line). Axons then extend adjacent to this substrate in a Dcc-dependent manner.

(T and U) Our conditional analyses support the growth substrate model, by demonstrating the key requirement for VZ-derived netrin1 in guiding spinal axons.

Data are represented as mean ± SEM. Probability of similarity, ***p < 0.0005, **p < 0.005, *p < 0.05, Student's t test. Scale bar is represented as 115 μm.

widely expressed in postmitotic neurons in the spinal cord (Figure S2A) and Dcc protein decorates a broad population of commissural axons (Figures S2D–S2F) (Phan et al., 2011). Of the Unc5 family, only *Unc5a* and *Unc5c* have detectable expression in postmitotic neurons in the spinal cord (Figures S2B and S2C) (Engelkamp, 2002; Leonardo et al., 1997; Masuda et al., 2008). Analysis of *Dcc*, *Unc5a*, and *Unc5c* mutants, demonstrated that only the loss of *Dcc* recapitulated all of the phenotypes seen in *netrin1*$^{lacZ/lacZ}$ mice to quantitatively similar amounts (Figures 4P, 1CC, and S2M). In the absence of *Dcc*,

NF^+ and $Robo3^+$ axons profusely project into the VZ (Figures 4M–4P) and $Robo3^+$ axons are highly defasciculated, extending throughout the motor column (Figure 4O). In contrast, $Robo3^+$ axon extension was not perturbed in the *Unc5a* and *Unc5c* mutants (Figures S2G–S2L and S2M). Together, these observations support the conclusion that Dcc is the key receptor in spinal commissural axons that orients their ventrally directed extension along the pial-netrin1 substrate and permits them to grow around the VZ.

DISCUSSION

Reassessing the Role of Netrin1 in the Spinal Cord

Netrin1 was first identified in a biochemical screen for soluble factors in chicken brain extracts that promote axon outgrowth (Kennedy et al., 1994; Serafini et al., 1994). Through these experiments, netrin1 became the prototypical example of a long-range diffusible chemoattractant, secreted by the FP (Figure 4Q). However, our studies support an alternative model: VZ-derived netrin1 acts as a growth substrate that promotes ventrally directed axonal growth by haptotaxis (Figure 4R) (MacLennan et al., 1997). Our conditional genetic analyses have distinguished between these models. Axon guidance defects are observed after netrin1 is removed from the VZ but not the FP (Figures 4T and 4U). Thus, FP-derived netrin1 is not required for commissural axon guidance.

Netrin1 belongs to the laminin superfamily, most closely resembling the laminin γ chain (Serafini et al., 1994), making it plausible that netrin1 functions within the context of the ECM. Our studies show that netrin1 closely associates with the laminin along the pial surface of the spinal cord, to establish a local growth substrate for axons. This result is consistent with previous studies demonstrating that netrin1 acts locally in other systems (Akin and Zipursky, 2016; Baker et al., 2006; Brankatschk and Dickson, 2006; Deiner et al., 1997; Timofeev et al., 2012). While our model is inconsistent with the observations that netrin1 appears to act as graded diffusible chemoattractant in in vitro assays, it is noteworthy that these assays usually require ECM components, such as laminin or collagen for axon extension (Hazen et al., 2010). These ECM factors might convert bath- or pipette-applied netrin1 into a tethered substrate for growth (Moore et al., 2012).

VZ-Derived Netrin1 Mediates Axon Growth in a Dcc-Dependent Manner

Our studies suggest that netrin1 functions as a growth substrate for axons in the developing spinal cord. We propose that this growth substrate is established when netrin1 protein made by bipolar neuroepithelial progenitors is transported to the lateral margins of the spinal cord via the basal progenitor endfeet, which contact the $laminin^+$ pial surface (Figure 4S) (Rousso et al., 2012). Pial-associated netrin1 both orients ventrally directed axon growth and promotes fasciculation. The mechanism by which the netrin1 promotes axon fasciculation remains unclear; however, it is intriguing that netrin1 appears to accumulate on axons after encountering pial-associated netrin in a Dcc-dependent manner. Thus, netrin1 is only observed on commissural axons as they enter the ventral spinal cord after the ablation of netrin1 from dorsal neural progenitors (Figure 4U). Moreover, axonal netrin1 is greatly diminished in *Dcc* mutants even though netrin1 is present at the pial surface. One possibility is that Dcc and netrin interact in *cis* in commissural axons to promote their fasciculated growth around the VZ (Figure 4S). Indeed, Netrin and Dcc (frazzled) have previously been suggested to interact within axons in *Drosophila*, to permit the en passant presentation of netrin to subsequent axons (Hiramoto et al., 2000).

The VZ-derived netrin1 guidance cue also appears to permit axons to grow precisely around domains of *netrin1* expression. This boundary activity was most notably observed after the focal loss of *netrin1* expression in the VZ using the Notch OFF approach. NF^+ axons deviate from their trajectories to follow the two ectopic borders of *netrin1* expression in the VZ (Figure 2EE). The mechanistic basis of this boundary requires further study. Is the $netrin1^+$ pial substrate an adhesive "go" surface that is sufficient to promote fasciculated axon growth, perhaps by "pulling" axons toward it and thereby out of the VZ? Or do the *netrin1*-expressing neural progenitors also represent a "no go" region which is actively avoided by axons?

Our studies suggest that many classes of spinal axons require netrin1 to avoid growing in the VZ. The $Tag1^+$ population of dorsal commissural axons may be an exception to this general rule. Neither $Tag1^+$ nor $Atoh1::taugfp^+$ (data not shown) commissural axons grow medially into the VZ as robustly as $Robo3/NF^+$ axons in *netrin1/Dcc* mutants, suggesting that additional factors may keep the dorsal-most dI1 axons from growing into the VZ. However, as with other populations of spinal axons, $Tag1^+$ axon outgrowth is not dependent on signals from the FP. Outgrowth defects are only observed when netrin1 is ablated either entirely (Figure 1W; Serafini et al., 1996) or specifically from the VZ (Figure 2O).

In summary, our studies show that FP-derived netrin1 is not required to direct axon growth, suggesting that netrin1 does not act as a diffusible chemotropic guidance signal for commissural axon guidance in the spinal cord. We propose that VZ-derived netrin1 provides an adhesive axon growth substrate to orient axon extension toward the ventral midline and promote axon fasciculation.

STAR★METHODS

Detailed methods are provided in the online version of this paper and include the following:

- KEY RESOURCES TABLE
- CONTACT FOR REAGENT AND RESOURCE SHARING
- EXPERIMENTAL MODEL AND SUBJECT DETAILS
  - Generation and analysis of mutant mice
- METHOD DETAILS
  - Immunohistochemistry
  - Antigen retrieval
  - Confocal Imaging and 3D rendering
  - In situ hybridization
- QUANTIFICATION AND STATISTICAL ANALYSIS
- DATA AND SOFTWARE AVAILABILITY

SUPPLEMENTAL INFORMATION

Supplemental Information includes two figures and three movies and can be found with this article online at http://dx.doi.org/10.1016/j.neuron.2017.03.007.

AUTHOR CONTRIBUTIONS

S.G.V. performed all experiments, with early assistance from S.C.P. J.H.K., K.D.P., T.-J.K, B.G.N., J.C., and A.K. provided tissue reagents. H.E. provided a mouse line. S.J.B. and S.G.V. conceived and designed the experiments with input from B.G.N. S.J.B. and S.G.V. wrote the manuscript.

ACKNOWLEDGMENTS

We are most grateful to Alex Joyner and Marc Tessier-Lavigne for the gifts of mutant mice and for Joe Herrold and Anna Maria Maglunog for early technical assistance. We would also like to thank James Briscoe, Greg Bashaw, Orkun Akin, and Larry Zipursky for invaluable discussions and comments on the manuscript. This work was supported by grants from the National Institute of Health (NIH) (DK097075, HL098294, HL114457, DK082509, HL109233, DK109574, HL119837, and HL133900) to H.E., Canadian Institutes of Health Research (MOP-97758 and MOP-77556), Brain Canada, Natural Sciences and Engineering Research Council, Canadian Foundation for Innovation, and the W. Garfield Weston Foundation to A.K., the March of Dimes Foundation (6-FY10-296) and National Institute of Health (NIH) (NS072804, NS089817, and NS085227) to B.G.N., and the March of Dimes (1-FY07-458), the NIH (NS063999 and NS085097), and the UCLA Broad Stem Cell Research Center to S.J.B.

Received: April 21, 2016
Revised: January 12, 2017
Accepted: February 22, 2017
Published: April 20, 2017; corrected online: May 2, 2017

REFERENCES

Ackerman, S.L., Kozak, L.P., Przyborski, S.A., Rund, L.A., Boyer, B.B., and Knowles, B.B. (1997). The mouse rostral cerebellar malformation gene encodes an UNC-5-like protein. Nature *386*, 838–842.

Akin, O., and Zipursky, S.L. (2016). Frazzled promotes growth cone attachment at the source of a Netrin gradient in the Drosophila visual system. eLife *5*, 5.

Baker, K.A., Moore, S.W., Jarjour, A.A., and Kennedy, T.E. (2006). When a diffusible axon guidance cue stops diffusing: roles for netrins in adhesion and morphogenesis. Curr. Opin. Neurobiol. *16*, 529–534.

Bielle, F., Griveau, A., Narboux-Neme, N., Vigneau, S., Sigrist, M., Arber, S., Wassef, M., and Pierani, A. (2005). Multiple origins of Cajal-Retzius cells at the borders of the developing pallium. Nat. Neurosci *8*, 1002–1012.

Brankatschk, M., and Dickson, B.J. (2006). Netrins guide Drosophila commissural axons at short range. Nat. Neurosci. *9*, 188–194.

Brunet, I., Gordon, E., Han, J., Cristofaro, B., Broqueres-You, D., Liu, C., Bouvrée, K., Zhang, J., del Toro, R., Mathivet, T., et al. (2014). Netrin-1 controls sympathetic arterial innervation. J. Clin. Invest. *124*, 3230–3240.

Butler, S.J., and Bronner, M.E. (2015). From classical to current: analyzing peripheral nervous system and spinal cord lineage and fate. Dev. Biol. *398*, 135–146.

Butler, S.J., and Tear, G. (2007). Getting axons onto the right path: the role of transcription factors in axon guidance. Development *134*, 439–448.

Carter, S.B. (1965). Principles of cell motility: the direction of cell movement and cancer invasion. Nature *208*, 1183–1187.

de la Torre, J.R., Höpker, V.H., Ming, G.L., Poo, M.M., Tessier-Lavigne, M., Hemmati-Brivanlou, A., and Holt, C.E. (1997). Turning of retinal growth cones in a netrin-1 gradient mediated by the netrin receptor DCC. Neuron *19*, 1211–1224.

Deiner, M.S., Kennedy, T.E., Fazeli, A., Serafini, T., Tessier-Lavigne, M., and Sretavan, D.W. (1997). Netrin-1 and DCC mediate axon guidance locally at the optic disc: loss of function leads to optic nerve hypoplasia. Neuron *19*, 575–589.

Dessaud, E., Yang, L.L., Hill, K., Cox, B., Ulloa, F., Ribeiro, A., Mynett, A., Novitch, B.G., and Briscoe, J. (2007). Interpretation of the sonic hedgehog morphogen gradient by a temporal adaptation mechanism. Nature *450*, 717–720.

Engelkamp, D. (2002). Cloning of three mouse Unc5 genes and their expression patterns at mid-gestation. Mech. Dev. *118*, 191–197.

Ericson, J., Morton, S., Kawakami, A., Roelink, H., and Jessell, T.M. (1996). Two critical periods of Sonic Hedgehog signaling required for the specification of motor neuron identity. Cell *87*, 661–673.

Fazeli, A., Dickinson, S.L., Hermiston, M.L., Tighe, R.V., Steen, R.G., Small, C.G., Stoeckli, E.T., Keino-Masu, K., Masu, M., Rayburn, H., et al. (1997). Phenotype of mice lacking functional Deleted in colorectal cancer (Dcc) gene. Nature *386*, 796–804.

Han, H., Tanigaki, K., Yamamoto, N., Kuroda, K., Yoshimoto, M., Nakahata, T., Ikuta, K., and Honjo, T. (2002). Inducible gene knockout of transcription factor recombination signal binding protein-J reveals its essential role in T versus B lineage decision. Int. Immunol. *14*, 637–645.

Harfe, B.D., Scherz, P.J., Nissim, S., Tian, H., McMahon, A.P., and Tabin, C.J. (2004). Evidence for an expansion-based temporal Shh gradient in specifying vertebrate digit identities. Cell *118*, 517–528.

Hazen, V.M., Phan, K., Yamauchi, K., and Butler, S.J. (2010). Assaying the ability of diffusible signaling molecules to reorient embryonic spinal commissural axons. J. Vis. Exp. (37), 1853.

Hiramoto, M., Hiromi, Y., Giniger, E., and Hotta, Y. (2000). The Drosophila Netrin receptor Frazzled guides axons by controlling Netrin distribution. Nature *406*, 886–889.

Hockfield, S., and McKay, R.D. (1985). Identification of major cell classes in the developing mammalian nervous system. J. Neurosci. *5*, 3310–3328.

Kadison, S.R., Murakami, F., Matise, M.P., and Kaprielian, Z. (2006). The role of floor plate contact in the elaboration of contralateral commissural projections within the embryonic mouse spinal cord. Dev. Biol. *296*, 499–513.

Kennedy, T.E., Serafini, T., de la Torre, J.R., and Tessier-Lavigne, M. (1994). Netrins are diffusible chemotropic factors for commissural axons in the embryonic spinal cord. Cell *78*, 425–435.

Kennedy, T.E., Wang, H., Marshall, W., and Tessier-Lavigne, M. (2006). Axon guidance by diffusible chemoattractants: a gradient of netrin protein in the developing spinal cord. J. Neurosci. *26*, 8866–8874.

Kolodkin, A.L., and Tessier-Lavigne, M. (2011). Mechanisms and molecules of neuronal wiring: a primer. Cold Spring Harb. Perspect. Biol. *3*, 3.

Kong, J.H., Yang, L., Dessaud, E., Chuang, K., Moore, D.M., Rohatgi, R., Briscoe, J., and Novitch, B.G. (2015). Notch activity modulates the responsiveness of neural progenitors to sonic hedgehog signaling. Dev. Cell *33*, 373–387.

Lai Wing Sun, K., Correia, J.P., and Kennedy, T.E. (2011). Netrins: versatile extracellular cues with diverse functions. Development *138*, 2153–2169.

Lang, D., Lu, M.M., Huang, L., Engleka, K.A., Zhang, M., Chu, E.Y., Lipner, S., Skoultchi, A., Millar, S.E., and Epstein, J.A. (2005). Pax3 functions at a nodal point in melanocyte stem cell differentiation. Nature *433*, 884–887.

Laumonnerie, C., Tong, Y.G., Alstermark, H., and Wilson, S.I. (2015). Commissural axonal corridors instruct neuronal migration in the mouse spinal cord. Nat. Commun. *6*, 7028.

Leonardo, E.D., Hinck, L., Masu, M., Keino-Masu, K., Ackerman, S.L., and Tessier-Lavigne, M. (1997). Vertebrate homologues of C. elegans UNC-5 are candidate netrin receptors. Nature *386*, 833–838.

MacLennan, A.J., McLaurin, D.L., Marks, L., Vinson, E.N., Pfeifer, M., Szulc, S.V., Heaton, M.B., and Lee, N. (1997). Immunohistochemical localization of netrin-1 in the embryonic chick nervous system. J. Neurosci. *17*, 5466–5479.

Mao, X., Fujiwara, Y., Chapdelaine, A., Yang, H., and Orkin, S.H. (2001). Activation of EGFP expression by Cre-mediated excision in a new ROSA26 reporter mouse strain. Blood *97*, 324–326.

Masuda, T., Watanabe, K., Sakuma, C., Ikenaka, K., Ono, K., and Yaginuma, H. (2008). Netrin-1 acts as a repulsive guidance cue for sensory axonal projections toward the spinal cord. J. Neurosci. *28*, 10380–10385.

Matise, M.P., Epstein, D.J., Park, H.L., Platt, K.A., and Joyner, A.L. (1998). Gli2 is required for induction of floor plate and adjacent cells, but not most ventral neurons in the mouse central nervous system. Development *125*, 2759–2770.

Matise, M.P., Lustig, M., Sakurai, T., Grumet, M., and Joyner, A.L. (1999). Ventral midline cells are required for the local control of commissural axon guidance in the mouse spinal cord. Development *126*, 3649–3659.

Ming, G.L., Song, H.J., Berninger, B., Holt, C.E., Tessier-Lavigne, M., and Poo, M.M. (1997). cAMP-dependent growth cone guidance by netrin-1. Neuron *19*, 1225–1235.

Moore, S.W., Zhang, X., Lynch, C.D., and Sheetz, M.P. (2012). Netrin-1 attracts axons through FAK-dependent mechanotransduction. J. Neurosci. *32*, 11574–11585.

Phan, K.D., Hazen, V.M., Frendo, M., Jia, Z., and Butler, S.J. (2010). The bone morphogenetic protein roof plate chemorepellent regulates the rate of commissural axonal growth. J. Neurosci. *30*, 15430–15440.

Phan, K.D., Croteau, L.P., Kam, J.W., Kania, A., Cloutier, J.F., and Butler, S.J. (2011). Neogenin may functionally substitute for Dcc in chicken. PLoS ONE *6*, e22072.

Poliak, S., Morales, D., Croteau, L.P., Krawchuk, D., Palmesino, E., Morton, S., Cloutier, J.F., Charron, F., Dalva, M.B., Ackerman, S.L., et al. (2015). Synergistic integration of Netrin and ephrin axon guidance signals by spinal motor neurons. eLife *4*, 4.

Rousso, D.L., Pearson, C.A., Gaber, Z.B., Miquelajauregui, A., Li, S., Portera-Cailliau, C., Morrisey, E.E., and Novitch, B.G. (2012). Foxp-mediated suppression of N-cadherin regulates neuroepithelial character and progenitor maintenance in the CNS. Neuron *74*, 314–330.

Serafini, T., Kennedy, T.E., Galko, M.J., Mirzayan, C., Jessell, T.M., and Tessier-Lavigne, M. (1994). The netrins define a family of axon outgrowth-promoting proteins homologous to C. elegans UNC-6. Cell *78*, 409–424.

Serafini, T., Colamarino, S.A., Leonardo, E.D., Wang, H., Beddington, R., Skarnes, W.C., and Tessier-Lavigne, M. (1996). Netrin-1 is required for commissural axon guidance in the developing vertebrate nervous system. Cell *87*, 1001–1014.

Sloan, T.F., Qasaimeh, M.A., Juncker, D., Yam, P.T., and Charron, F. (2015). Integration of shallow gradients of Shh and Netrin-1 guides commissural axons. PLoS Biol. *13*, e1002119.

Tessier-Lavigne, M., and Goodman, C.S. (1996). The molecular biology of axon guidance. Science *274*, 1123–1133.

Timofeev, K., Joly, W., Hadjieconomou, D., and Salecker, I. (2012). Localized netrins act as positional cues to control layer-specific targeting of photoreceptor axons in Drosophila. Neuron *75*, 80–93.

Williams, M.E., Lu, X., McKenna, W.L., Washington, R., Boyette, A., Strickland, P., Dillon, A., Kaprielian, Z., Tessier-Lavigne, M., and Hinck, L. (2006). UNC5A promotes neuronal apoptosis during spinal cord development independent of netrin-1. Nat. Neurosci. *9*, 996–998.

STAR★METHODS

KEY RESOURCES TABLE

REAGENT or RESOURCE	SOURCE	IDENTIFIER
Antibodies		
Rabbit anti-Neurofilament, 1:200	Cell Signaling Technology	Cat#C28E10; RRID: AB_10828120
Rabbit anti-Shh, 1:200, H4	Ericson et al., 1996	N/A
Rabbit anti-Laminin, 1:1000	Abcam	Cat#Ab11575; RRID: AB_298179
Goat anti-human Robo3, 1:200	R&D Systems	Cat#AF3076; RRID: AB_2181865
Goat anti-mouse Dcc, 1:500	R&D Systems	Cat#AF844; RRID: AB_2089765
Goat anti-mouse Netrin1, 1:500	R&D Systems	Cat#AF1109; RRID: AB_2298775
Goat anti-β-galactosidase, 1:2000	Biogenesis	Cat#4600-1409
Goat anti-Sox2, 1:2000	Santa Cruz Biotechnology	Cat#17320; RRID: AB_2286684
Mouse anti-cre, 1:1000	Covance	Cat#MMS-106P; RRID: AB_10064070
Mouse anti-Sox2-E4, 1:1000	Santa Cruz Biotechnology	Cat#365823; RRID: AB_10842165
Mouse monoclonal anti-Tag1, 1:100	DSHB	Cat#4D7; RRID: AB_2315433
Mouse anti-Neurofilament, 1:100	DSHB	Cat#3A10; RRID: AB_531874
Mouse anti-Rat Nestin, 1:50	DSHB	Cat#Rat-401; RRID: AB_2235915
Chicken anti-GFP, 1:1000	Aves Lab	Cat#1020; RRID: AB_10000240
Chicken anti-Neurofilament, 1:2000	Millipore	Cat#Ab5539; RRID: AB_177520
Experimental Models: Organisms/Strains		
Mouse: Netrin1-lacz gene trap	Serafini et al., 1996	N/A
Mouse: Dcc	Fazeli et al., 1997	N/A
Mouse: Gli2	Matise et al., 1998	N/A
Mouse: Unc5a	Williams et al., 2006	N/A
Mouse: Unc5c	Ackerman et al., 1997	N/A
Mouse: Dbx1::cre	Bielle et al., 2005	N/A
Mouse: Olig2::cre	Dessaud et al., 2007	N/A
Mouse: Rosa26R::GFP,	Jackson Laboratories	RRID: IMSR_JAX:004077
Mouse: Rbpj flox/flox	Han et al., 2002	n/a
Mouse: Shh::cre	Jackson Laboratories	RRID: IMSR_JAX:005622
Mouse: Pax::cre	Jackson Laboratories	RRID: IMSR_JAX:005549
Mouse: Netrin1 flox/flox	Brunet et al., 2014	N/A
Oligonucleotides		
In situ probe for Unc5a: forward 5′-TGAAGTTGTCCCTC GATGCT-3′, reverse 5′- GACATTAACCCTCACTA AAGGGAGTGATCGTGTGCCTGAATCC-3′, T3 site	This paper	N/A
In situ probe for Unc5c: forward 5′- CCTTTGCCCATT TCTGTGTT-3′, reverse 5′- GACTAATACGACTCACTAT AGGGAGAAGACAGCAGGAGGGTGA-3′, T7 site	This paper	N/A
In situ probe for Dcc: forward 5′- GAGTATTTAGGTGA CACTATAG-3′, reverse 5′-GACTATTTAGGTGACACTATA GGACACAATCAGCAGCAGGAA-3′, SP6 site	Phan et al., 2011	N/A
Software and Algorithms		
Zen Black	Carl Zeiss	2012
Adobe Photoshop	Adobe	CS6
Imaris XT	Bitplane	Imaris x64 v8.3, http://bitplane.com/
Primer3	Primer3 program	http://primer3plus.com

CONTACT FOR REAGENT AND RESOURCE SHARING

Further information and requests for resources and reagents should be directed to the Lead Contact, Samantha Butler (butlersj@ucla.edu).

EXPERIMENTAL MODEL AND SUBJECT DETAILS

Generation and analysis of mutant mice

Netrin1 (Serafini et al., 1996), *Dcc* (Fazeli et al., 1997), *Gli2* (Matise et al., 1998) mice were bred into 129/Sv backgrounds; *Unc5a* (Williams et al., 2006), *Unc5c* (Ackerman et al., 1997), Dbx1::*cre* (Bielle et al., 2005), Olig2::*cre* (Dessaud et al., 2007; Kong et al., 2015), Rosa26R::*gfp* (Mao et al., 2001), *Rbpj*$^{flox/flox}$ mice (Han et al., 2002), *Netrin1*$^{flox/flox}$ mice (Brunet et al., 2014)), Shh::*cre* (Harfe et al., 2004) and Pax3::*cre* (Lang et al., 2005) were maintained in C57BL/6 backgrounds. The *netrin1* mutant strain stems from *lacZ* having been inserted into the *netrin1* genomic locus and is considered to be a hypomorphic allele (Serafini et al., 1996). While there are trace amounts of residual *netrin1* expression in *netrin1*$^{lacZ/lacZ}$ FPs, there is no detectable *netrin1* transcript in the *netrin1*$^{lacZ/lacZ}$ VZ at any stage (Figures S1C) or any detectable netrin1 protein at either the pial surface or on spinal axons (Figure 4E). Note that as previously described (Poliak et al., 2015; Serafini et al., 1996), netrin1 antibodies detect both the endogenous protein associated with cell membranes and the netrin1::β-gal fusion protein, which accumulates in the cytoplasm of mutant cells.

Mice were handled and housed in accordance with the University of California Los Angeles IACUC guidelines. Embryos were derived from timed matings with heterozygous mice. The day of the plug was counted as E0.5, and embryos were harvested at E11.5. Notch OFF mice were generated by crossing Dbx1::*cre* mice with *Rbpj*$^{flox/flox}$ mice, as previously described (Kong et al., 2015). Netrin1 conditional knockout embryos were generated by crossing Shh::*cre* or Pax3::*cre* drivers with *netrin1*$^{flox/flox}$ mice. *Netrin1*$^{lacZ/lacZ}$, *Unc5c* and *Dcc* analyses used littermate wild-type controls, except in the case of *Unc5a* mice, which were bred as homozygous mutants and compared to *Unc5c* wild-type controls. All the conditional knockout analyses used heterozygous floxed littermates as controls. Genotypes were identified by PCR reactions using cDNA for *netrin1*$^{lacZ/lacZ}$ embryos and genomic DNA for all other lines.

METHOD DETAILS

Immunohistochemistry

Mouse embryonic spinal cords (E10.5-E12.5) were fixed in 4% paraformaldehyde for 2 hr at 4°C, cryoprotected in 30% sucrose in PBS overnight and thin-sectioned to yield 30μm transverse sections. Antibody staining was performed by incubating the sections with primary antibodies at 4°C overnight, followed by fluorescently-labeled secondary antibodies at room temperature for 2 hr. Antibodies against the following proteins were used for immunostaining: *Rabbit:* neurofilament (NF), 1:200 (Cell Signaling Technology C28E10); Shh, 1:200 (H4 (Ericson et al., 1996)); Laminin, 1:1000 (Abcam #ab11575); *Goat:* human Robo3, 1:200 (R&D Systems AF3076); mouse Dcc, 1:500 (R&D Systems AF844); mouse netrin1, 1:500 (R&D Systems AF1109); β-galactosidase, 1:2000 (Biogenesis 4600-1409); Sox2, 1:2000 (Santa Cruz Biotechnology #17320); *Mouse:* cre, 1:1000 (Covance MMS-106P); Sox2, 1:1000 (Santa Cruz Biotechnology #365823); mAb Tag1 1:100 (4D7, Developmental Studies Hybridoma Bank (DSHB)); NF, 1:100 (3A10 DSHB); Nestin, 1:50 (Rat-401 DSHB); *Chicken:* GFP, 1:1000 (Aves Lab #1020); neurofilament, 1:2000 (Millipore #AB5539). Secondary antibodies (all from Jackson Immunoresearch Laboratories) were used as follows: FITC, 1:500; Alexa488, 1:1000; Cyanine3, 1:1000; Cyanine5 1:700.

Antigen retrieval

The netrin1 antibody signal was augmented using standard antigen retrieval techniques. Slides were post-fixed with 4% paraformaldehyde for 10 min, rinsed with PBS, and boiled in a 10mM sodium citrate buffer (pH 6.0) for 3 min in a microwave. Slides were allowed to cool in the buffer solution for 20 min at room temperature, before processing for immunohistochemistry. All netrin1 immunostaining was performed with antigen retrieval except when used with antibodies that were affected by the retrieval method; for example, Tag1 antigenicity was completely lost, while laminin antigenicity was moderately affected post-retrieval. The netrin1 staining in Figure 3G was performed without retrieval to preserve the antigenicity of the sample. Netrin1 protein is most readily observed after antigen retrieval methods. See Figures 3C and 3G for a respective comparison with and without antigen retrieval; the specificity of the netrin1 antibody is demonstrated in Figures 4B and 4E.

Confocal Imaging and 3D rendering

Images were acquired on Carl Zeiss LSM700, LSM800 and LSM880 with Airyscan confocal microscopes and processed using Carl Zeiss Zen 2012 and Adobe Photoshop CS6 software. Imaris x64 v8.3 and Imaris XT software from Bitplane Inc (http://bitplane.com/) were used to render 3d models of images. Movies S1, S2, and S3 were processed using Imaris and Imaris XT: the 'spots' function was used to render 3D models of netrin1 protein while the 'surfaces' function was used to render 3D models of nestin and NF. A threshold for intensity sum was used for each channel and spots were further classified with respect to distance from each surface using the 'spots close to surface' MATLAB Imaris XTension.

In situ hybridization

Digioxigenin (DIG) labeled probes against the 3′ untranslated regions of genes of interest were generated using the Roche RNA Labeling Kit and were used on 12μm transverse sections. mRNA signal was visualized using NBT/BCIP and anti-DIG antibody conjugated with an alkaline phosphatase fragment (Roche). Target sequences were amplified using cDNA from mouse embryonic spinal cord using the following primers that were designed with the Primer 3 program (http://primer3plus.com/):

Unc5A: forward 5′-TGAAGTTGTCCCTCGATGCT-3′, reverse 5′- GACATTAACCCTCACTAAAGGGAGTGATCGTGTGCCTGAATCC-3′;
Unc5C: forward 5′- CCTTTGCCCATTTCTGTGTT-3′, reverse 5′- GACTAATACGACTCACTATAGGGAGAAGACAGCAGGAGGGTGA-3′;

The underlined text denotes either a T3 or T7 polymerase binding site. Dcc and netrin1 probes were described previously (Phan et al., 2011) (Serafini et al., 1996).

QUANTIFICATION AND STATISTICAL ANALYSIS

No statistical methods were used to predetermine sample sizes, but these were similar to those in our previous publications (Phan et al., 2010). All quantifications were performed blind. Data were tested for normality and compared using a 2-paired 2-tail Student's t test. Probability of similarity, *** $p < 0.0005$, ** $p < 0.005$, * $p < 0.05$. Variance was similar between groups being compared. n represents number of sections in all cases; for each experiment sections were analyzed and pooled together from multiple embryos from more than one litter. Data is represented as mean ± SEM.

DATA AND SOFTWARE AVAILABILITY

All statistics and graphs were generated using Microsoft Excel and Graphpad Prism6 software. See Key Resources Table for information regarding other softwares used.